Sensors and Materials, Vol. 14, No. 4 (2002) 179–187
MYU Tokyo

S & M 0480

Use of Laser Scanning Cytometry for Analysis of Endothelial Cells Attached to Micropatterned Silicon Surfaces

Nicanor I. Moldovan[1, 2*], Sumant S. Kulkarni[1] and Mauro Ferrari[1, 2]

[1]Biomedical Engineering Center, [2]Davis Heart and Lung Research Institute,
The Ohio State University, Columbus, OH 43210, U.S.A.

(Received October 12, 2001: accepted December 18, 2001)

Key words: microdevice/cell array, microfabrication, laser scanning cytometer, endothelial cells, morphology, quantification

The development of microdevices with biomedical applications relies on the understanding of cell behavior at bioinorganic interfaces. Micropatterning of these surfaces for controlled cell attachment is known to strongly influence cellular physiology. However, an integrated platform for the analysis of the correlation between the physiological status of the living cells and their topographical parameters on a micron scale has not been available to date. Here, we suggest that laser scanning cytometry (LSC), a newly developed solid-state flow cytometry-like technology, offers an attractive solution. We also provide the proof of concept for its application in the analysis of endothelial cells grown in micron-width bands on the surface of silicon wafers. We used LSC analysis to compare the growth of endothelial cells on line patterned and nonpatterned areas, in terms of several nuclear morphological parameters. Our data support the conclusion that lateral confinement of endothelial cell attachment induces a quiescent state, possibly by inhibiting their ability to proliferate.

1. Introduction

The interaction between electronics engineers, material scientists and biologists has produced a new breed of biomedical engineering. In this novel area, microfabrication technologies, hitherto specific to the electronics industry, are used to develop novel analytical cell arrays, implantable biosensors, biostimulators, drug delivery microsystems,

*Corresponding author, e-mail address: moldovan-1@medctr.osu.edu

tissue engineering-based biomedical micro/nanodevices, and so forth.[1] A central theme in this field has been the satisfactory micropatterning of cells.[2] In this respect, researchers are investigating the behavior of cells on substrates that have been pre-patterned by micro/nanofabrication. Thus, it was shown that cell physiology can be controlled by the amount and shape of its adhesive substrate.[1–3]

Cellular responses to topography have been extensively considered in the past. For example, some properties of various cell types (*e.g.*, fibroblasts[4,5]), can be influenced solely by their response to microtopographically patterned substrates.[6] Biocompatibility of various materials is modulated by the presence of a specific topography on the nearby surface[7]; (see also Folch and Toner[8] for a thorough review of cellular interactions with surfaces microfabricated to reproduce biological environments).

Several techniques of micropatterning such as 'soft lithography'[9–11] have been developed with biological applications in mind. However, with few exceptions[11] most studies along these lines have focused only on the fabrication of the substrates and the successful attachment of cells, but usually stop short of a comprehensive analysis of physiological responses of the cells in those conditions. The reason for the slow progress in this domain is not the lack of interest, but the absence of an adequate, efficient experimental setting enabling the assessment of the biological effects of micropatterning.

We suggest here that a suitable approach fulfilling those needs is the laser scanning cytometer (LSC).[12] The LSC combines the benefits of flow cytometry with those of image-based cytometry into a single platform. In a short period of time, many innovative applications for the instrument have already been found. It has been used extensively for the analysis of the phenomenon of apoptosis.[13–15] Cancer researchers have considered it to perform Comet assays for DNA damage,[16] and for tumor content analysis.[17] It has also successfully been adapted in the fields of cell cycle analysis,[18] gene therapy,[21] immunofluorescence,[19] drug development and toxicology.[20]

In this paper, we demonstrate the benefits of LSC analysis of cells that have been patterned on a surface bearing well-defined microtopographical features (parallel bands and grooves). We recently discovered a critical role of local microtopography in the development of compensatory neo-angiogenesis in experimental cardiac ischemia.[21] In order to take advantage of this phenomenon, and to analyze the potential role of microtopography in the development of capillary-like structures *in vitro*, here we used standard photolithography and surface micromachining techniques to produce patterned regions of lines of various sizes in silicon wafers. These patterns were seeded with endothelial cells (EC) that were allowed to grow, and then fixed, incubated with the nuclear stain propidium iodide (PI), visualized by fluorescence microscopy, and examined by LSC. This analysis revealed that the patterned cells had different morphologies from those that adhered on unpatterned silicon. The results confirm the feasibility of the microvascular tissue engineering approach, and serve to highlight the capabilities of the LSC technology for the combined microscopic and quantitative analysis of large plain or micropatterned surfaces covered with cells.

2. Materials and Methods

2.1 *Endothelial cell culture and seeding*

Confluent mouse aortic endothelial cell (MAEC) monolayers[22] grown in T-75 tissue culture flasks (BD Falcon) were dissociated by a 5-min exposure to 5 ml of trypsin-EDTA (0.25%w/v, GibcoBRL Labs). The excess trypsin-EDTA was neutralized with an equal quantity of growth medium, consisting of DMEM (GibcoBRL) supplemented with 10% fetal bovine serum (GibcoBRL) and a mixture of antibiotics (100 U/ml penicillin, 100 μg/ml streptomycin and 0.25 μg/ml amphotericin). The cell suspension was centrifuged for 5 min at 4°C and 1100 rpm. The cell pellet thus obtained was re-suspended in the growth medium. The cell suspension thus obtained was used for seeding of the micropatterned silicon (Si) wafers.

The wafers were (1,0,0) Si crystals of industrial quality. 4-inch Si wafers with patterned regions of grooves were fabricated using standard photolithographic techniques. Each wafer bore several patterned regions of about 1 cm^2 each that consisted of grooves with progressively wider widths of 5, 10, 20, 50 and 80 μm. Groove spacing was equal to the width, and wafers with 20, 50 and 80 μm groove depths were employed.

For cell seeding, all wafers were sterilized by immersion in 70% ethanol for 24 h. The wafers were then rinsed three times in phosphate buffered saline (PBS, GibcoBRL), and then soaked for 2 h in PBS prior to seeding. A seeding density of 3.0×10^4 cells/cm^2 was chosen for covering the patterned or unpatterned wafer domains used here. The MAEC suspension was divided into a number of equal aliquots identical to the number of distinct patterned regions on the wafer. Each aliquot of MAEC suspension was then seeded frontally onto the patterned regions on each wafer, and allowed to settle for 2 h. Thereafter, growth medium was added to cover the wafers after the initial adhesion period. In all instances, the cells were cultured for an additional period of 48 h at 37°C and 5% CO_2 prior to fixing and staining. Unpatterned Si regions neighboring the grooved regions were also seeded with cells, which were used as controls.

2.2 *Fixing and staining procedure*

The cells seeded on the wafers were fixed with 100% ethanol at –20°C for 30 min. These cells were then exposed to RNAse A (USB Corp., 81.4 U/mg, 0.1 mg/ml) and stained with the nuclear stain propidium iodide (PI, Molecular Probes, Eugene, Oregon) at 1 μg/ml, for a further 30 min. Rectangular Si wafer bits with fixed and stained cells were then rinsed with PBS, mounted on glass slides, and cover-slipped.

2.3 *Laser scanning cytometer analysis*

LSC uses Ar and He-Ne lasers to excite the fluorescence of some of the widely used dyes in cell biology. It does so by emitting laser light through a microscope objective, onto a specimen that has been placed on its electronically controlled stage, and can collect both epifluorescence measurements using four optical filters and photomultiplicators (PMTs), and forward scatter using a solid-state sensor. The most important advantage of the LSC is that specimens are prepared on a slide and their position relative to the motorized stage is fixed, which lends it the unique capability to record cell position data that can later be used

to image events of interest. Moreover, by maintaining consistent positioning of the slide on the auto-stage, multiple, real-time data on the same cell sample can be acquired. Hence, unlike flow cytometry, the cell sample can be analyzed spatio-temporally, and the information on cell morphology can be recorded and retrieved for further evaluation and correlation.

We used the LSC instrument (CompuCyte Corp., Cambridge, MA), to analyze the Si wafer bits that contained the fixed, stained and mounted cell samples. The Olympus BX50 fluorescence microscope (Olympus Co. Tokyo, Japan), a part of the LSC system, was also used to view the cells, and a Kodak Digital Camera (DC120, Kodak Corp, Rochester, NY) attached to the microscope was used to acquire images of the fluorescent cells. Slides were scanned using the 20X objective and the 488 nm argon laser line, with 0.2 μm resolution. The scan area was adjusted such that it comprised the regions of the wafer that bore both patterned and unpatterned areas of interest. PI (red) fluorescence at 625 ± 28 nm was recorded by the use of the PMT and digitized signals were saved in the PC RAM. Contouring was performed using the PI parameter and the WinCyte software program was set up in such a way as to automatically contour the stained nuclei by means of specifying threshold values above which an event was considered to have occurred. Scanned cell data files were analyzed using the LSC WinCyte Software (CompuCyte Corp. Cambridge, MA). A specific subroutine may be activated to eliminate accidental overlaps between cells, called "multiple cell events".

3. Results and Discussion

In the present study, we analyzed by LSC the cellular responses with respect to microtopography, in the absence of other substrate-derived biochemical stimuli. This is an important relationship in the quest for the optimal design of implantable microdevices, because the biocompatibility of implants is known to depend on the material's micro- and nano-texture,[23] on the density of nearby microvessels,[24] and on its endothelialization.[25] In order to increase the biocompatibility and to prepare the implant surface with pre-made capillary-like structures,[26] we are interested in pre-assembling EC on micropatterned Si surfaces, in the size range of blood microvessels (tens of microns).

Here we report the successful EC micropatterning in response to the surface topography of the substrate (Fig. 1). This linear pattern was achieved simply by cell adhesion on the grooved domains, without providing the cells with any prior or concurrent biological or chemical stimulus for alignment. The only signal they could detect was the presence or absence of the grooves on the surface of the Si wafer. The response was found constantly and independently of the groove depth and width. However, the patterning effect was more pronounced with larger distances between grooves (50 and 80 μm).

Figure 1 shows a scattergram of the X-Y position of the cells. Polygonal sub-regions, outlined in gray tones on the figure, encompassed the regions and events of interest that were also created using the WinCyte software. This scattergram shows that cell patterning was indeed produced, and it was further confirmed by the fluorescence microcopy images taken from the same regions, with the same microscope (Fig. 1, inserts). As expected, neighboring unpatterned Si areas showed no such arrangement of the cells.

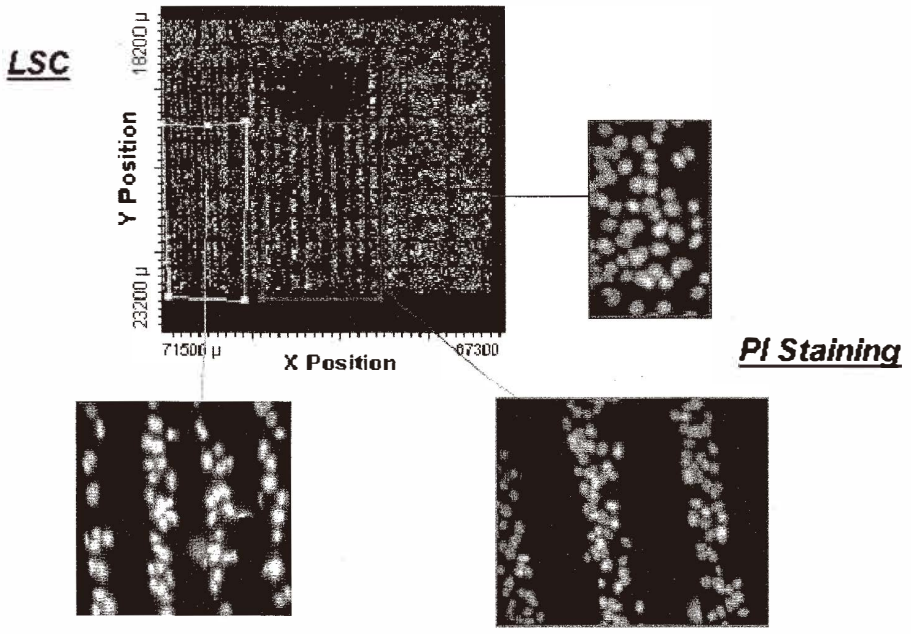

Fig. 1. Growth of mouse aortic endothelial cells on micropatterned silicon. LSC: the laser scanning cytometer scattergram recording of the position of each cell in adjacent patterned (50 and 80 μm wide ridges) and non-patterned domains of the same wafer, based on the propidium iodide (PI) staining of endothelial cells nuclei (attached inserts, not to scale). Note the ability of this assay to detect a seeding defect (the bare region on top of the selected area), which was excluded from further analysis.

The usefulness of LSC analysis is shown in Figs. 2 and 3, where the positional information is combined with the PI fluorescence (indicative of the nuclear size and compactness, both related to the cell cycle). For example, in Fig. 2, we could detect by LSC a significant dependence on the region of growth of the apparent nuclear brightness (Fig. 2C, PI integral vs. X position) and in cross-sectional nuclear area (Fig. 2D, area vs. X position) of the cells cultured on micropatterned Si. A bivariate distribution of both these parameters was found (Figs. 2C and 2D, arrows). This property was better displayed by the histograms presented in Fig. 3: the amplitude of the second peak, suggestive of cell division, was largest in the unpatterned region, reduced in the 80 μm bands domain, and almost absent in the region with 50-μm-wide bands.

Using the graphics facility of WinCyte software, we defined the domains containing the two peaks in the unpatterned region (Fig. 3B), and obtained the region's statistics. From it, we derived the mean area of the nuclei in the first (basal) peak as being 183±26.8 μm^2, while the area of the cells in the second peak was 308±32.8 μm^2, which suggests the presence of dividing cells in this population. In the two adjacent micropatterned regions,

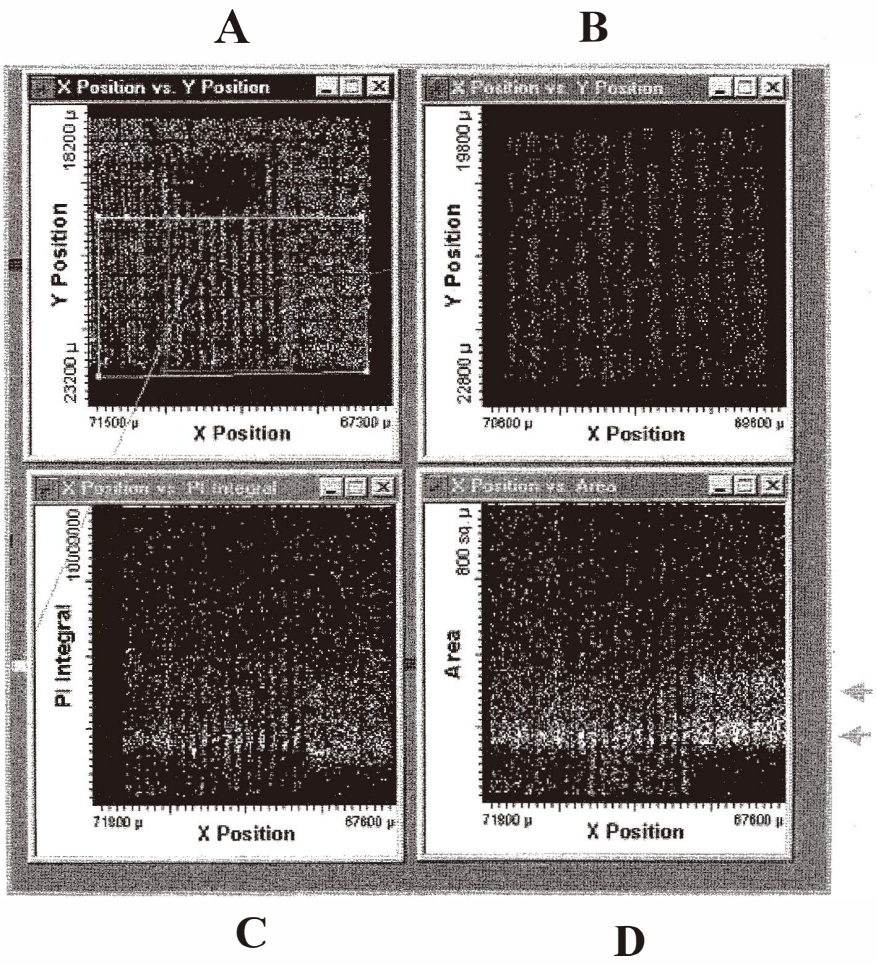

Fig. 2. LSC analysis of the cells on micropatterned silicon (same sample as in Fig. 2). A), B) X-Y recordings, C) PI fluorescence integral vs. X position; D) PI area vs. X. position are presented. In B), a magnified image of the 80 μm region is displayed. Note the bimodal distribution of the area and integral parameters, (C, D, arrows), depending on the patterning of the substrate.

the second peak was much less represented, indicating a more uniform nuclear distribution, and consequently, less cell division. The presence of a replicating cell sub-population on the unpatterned region was confirmed by means of the total fluorescence intensity in the two peaks (2,028,710 and 3,913,267 respectively, in arbitrary units) for these nuclei.

We further checked if the cross-sectional area and apparent total fluorescence intensity (i.e., PI integral, a measure of the quantity of bound chromophore) were directly propor-

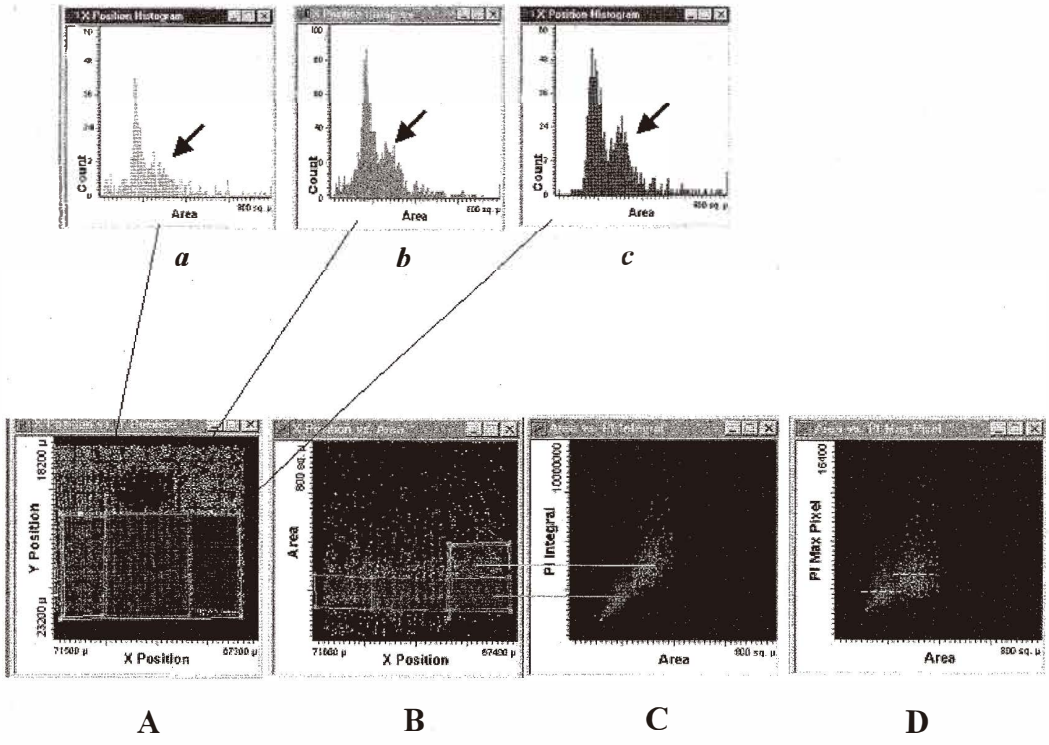

Fig. 3. Refined analysis of the bimodal distribution of cross-sectional nuclear areas of endothelial cell nuclei. a)-c) Histograms corresponding to the 50 μm, 80 μm and non-patterned domains. The arrows indicate the second (mitotic+G_2) peak, which decreases with the lateral restraint of the cells. The cells were analyzed in "multiple cell exclusion" mode. A) The source scattergram for a)-c). B) Definition of the domains considered for statistical analysis, area- PI integral, and area-PI maximum pixel correlations. C) Area- PI integral plot, showing a good linear correlation in the non-dividing nuclear population (dark gray) and increased brightness in the dividing nuclei (light gray). D) The area-max pixel correlation plot, which shows an increased brightness of the nuclei in the mitotic sub-population (light gray), vs. the quiescent cells (dark gray).

tional, in order to see if they reflect the same morphological reality. We found this to be the case in the non-dividing nuclei, while the total fluorescence intensities tended to be higher in the second nuclear peak (Fig. 3C). The increased relative PI brightness in the nuclei of the second peak may be interpreted as being related to the modified chromatin structure of mitotic cells.[13] Indeed, an increased chromatin condensation was reflected in the plot of area vs. PI maximum pixel (Fig. 3D), which clearly shows that the two cell groups have different maximal brightness. The associated medians were 3771 and 5003 (in arbitrary units).

The current data are in agreement with the conclusions of another study,[11] which showed that the limitation of lateral space for growth shuts off the proliferative program of EC, and induces their differentiation. When the available area became even smaller, the cells tended to enter apoptosis, a process likely to occur in our experimental model as well (Fig. 2C and 2D, the events below arrow level).

To our knowledge, this is the first instance where LSC has been used to analyze substrates bearing patterned cells on their surface. We chose Si as the substrate since it is highly compatible with the various microfabrication technologies that are extensively used in the electronics industry. It is also easy to integrate electronics into a Si chip and this could facilitate the successful manufacture of complex, multi-purpose implantable biodevices. Otherwise, LSC can collect events from any surface, of different mechanical properties, transparent or not, even if the cells do not adhere, but simply settle dispersed enough to be individually detected.

There are many advantages of using the LSC in the analysis of cells on micropatterned surfaces: a) it provides an accurate recording of cell positions, produced by micropatterning; b) it allows the collection of quantitative physiological parameters from the cellular population; c) it can easily perform correlation between different recorded parameters and images; d) it allows direct microscopic access to each individual event (cell) considered; e) it can analyze a large number of cells, thus allowing a thorough statistical analysis, or quality assessment.

Similar demands in the field of high throughput/content drug discovery and cell scanning have fuelled the development of systems such as the CellChip(TM).[27] However, this platform does not seem suitable for the analysis of micropatterns, due to its pre-configured geometry as a microplate reader, and to the fact that each experimental point, obtained from a well, is in fact a small collection of cells.

Microfabrication and micropatterning are likely to become important technological components in the manufacture of implantable biomedical microdevices, and of biosensors. Consequently, their successful implementation will create the need for a faster and more efficient assessment of the cell responses at the interface with these surfaces. Here it was demonstrated that the LSC may provide a convenient analysis platform for better understanding the biological phenomena on micropatterned surfaces.

Acknowledgments

This work was supported in part by the Shannon Award (RR13370) from NIH (Dr. Ferrari), and by the NIH RO1 HL65983 (Dr. Moldovan). The authors would like to thank Reid Orth (Cornell Nanofabrication Facility) and Dr. Jennifer Lewis for kindly providing us with the patterned Si wafers, Dr. R. Auerbach for the mouse aortic endothelial cells, and Dr. Derek Hansford for suggestions on the analysis of LSC data.

References

1 S. N. Bhatia and C. S Chen: Biomed. Microdevices **2** (1999) 131.
2 Y. Ito: Biomaterials **20** (1999) 2333.
3 C. S. Chen, M. Mrksich, S. Huang, G. M. Whitesides and D. E Ingber: Science **276** (1997) 1425.
4 A. M. Green, J. A. Jansen, J. P. C. M. van der Waerden and A. F von Recum: J. Biomed. Mater. Res. **28** (1994) 647.
5 J. Meyle, K. Gueltig, Wolburg, H. and A. F von Recum: J. Biomed. Mater. Res. **27** (1993) 1553.
6 A. Curtis and C. Wilkinson: Biomaterials **18** (1998) 1573.
7 E. T. den Braber, J. E. de Ruijter, L. A. Ginsel, A. F. von Recum and J. A Jansen: Biomaterials **17** (1996) 2037.
8 A. Folch and M. Toner: Annu. Rev. Biomed. Eng. **2** (2000) 227.
9 Y. Xia and G. M. Whitesides: Polym. Mater. Sci. Eng. **77** (1997) 596.
10 R. S. Kane, S. Takayama, E. Ostuni, D. E. Ingber and G. M. Whitesides: Biomaterials **20** (1999) 2363.
11 L. E. Dike, C. S Chen, M. Mrksich, J. Tien, G. M. Whitesides and D. E. Ingber: In Vitro Cell Dev Biol Anim. **35** (1999) 441.
12 L. A. Kamentsky and L. D. Kamentsky: Cytometry. **12** (1991) 381.
13 E. Bedner, X. Li, W. Gorczyca, M. Melamed and Z. Darzynkiewicz: Cytometry. **35** (1999) 181.
14 Z. Darzynkiewicz, E. Bedner, F. Traganos and T. Murakami: Hum Cell. **11** (1998) 3.
15 T. Furuya, T. Kamada, T. Murakami, A. Kurose and K. Sasaki: Cytometry. **29** (1997) 173.
16 A. B. Petersen, R. Gniadecki and H. C. Wulf: Cytometry. **39** (2000) 10.
17 W. Gorczya, Z. Darzynkiewicz and M. Melamed: Acta Cytol. **41** (1997) 98.
18 G. Juan and Z. Darzynkiewicz: Cell Biol. **2** (1998) 261.
19 M. Musco, S. Cui, D. Small, M. Nodelman, B. Sugarman and M. Grace: Cytometry. **33** (1998) 290.
20 R. J. Clatch and J. R. Foreman: Cytometry. **34** (1998) 36.
21 N. I. Moldovan, P. J. Goldschmidt-Clermont, J. Parker-Thornburg, S. Shapiro and P. Kolattukudy: Circ. Res. **87** (2000) 378.
22 M. Bastaki, E.E. Nelli, P. Dell'Era, M Rusnati, M. P. Molinari-Tosatti, S. Parolini, R. Auerbach, L. P. Ruco, L. Possati and M. Presta: Arterioscler. Thromb. Vasc. Biol. **17** (1997) 454.
23 U. Nydegger, R. Rieben and B. Lämmle: Transfusion Science **17** (1996) 481.
24 C. J. Kirkpatrick, M. Otto, T. Kooten, V. Van, Krump, J. Kriegsmann and F. J. Bittinger: J. Mater. Sci.: Materials in Medicine **10** (1999) 589.
25 R. A. Smith, M. W. Mosesson, A. U. Daniels and T. K Gartner: J. Mater. Sci.: Materials in Medicine **11** (2000) 279.
26 N. I. Moldovan and M. Ferrari: Arch. Pathol. Lab. Med. (2001) in press.
27 R. Kapur, K. A. Giuliano, M. Campana, T. Adams, K. Olson, D. Jung, M. Mrksich, C. Vasudevan and D. L. Taylor: Biomedical Microdevices **2** (1999) 99.